THE RELATIONSHIP BETWEEN THE 'LIMITING' YARKOVSKY DRIFT SPEED AND ASTEROID FAMILIES' YARKOVSKY V-SHAPE

I. Milić Žitnik

Astronomical Observatory, Volgina 7, 11000 Belgrade, Serbia

E–mail: *ivana@aob.rs*

SUMMARY: The Yarkovsky effect is an important force to consider in order to understand the long-term dynamics of asteroids. This non-gravitational force affects the orbital elements of objects revolving around a source of heat, especially their semi-major axes. Following the recently defined 'limiting' value of the Yarkovsky drift speed at 7×10^{-5} au/Myr in Milić Žitnik (2019) (below this value of speed asteroids typically jump quickly across the mean motion resonances), we decided to investigate the relation between the asteroid family Yarkovsky V-shape and the 'limiting' Yarkovsky drift speed of asteroid's semi-major axes. We have used the known scaling formula to calculate the Yarkovsky drift speed (Spoto et al. 2015) in order to determine the inner and outer 'limiting' diameters (for the inner and outer V-shape borders) from the 'limiting' Yarkovsky drift speed. The method was applied to 11 asteroid families of different taxonomic classes, origin type and age, located throughout the Main Belt. Here, we present the results of our calculation on relationship between asteroid families' V-shapes (crossed by strong and/or weak mean motion resonances) and the 'limiting' diameters in the $(a, 1/D)$ plane. Our main conclusion is that the 'breakpoints' in changing V-shape of the very old asteroid families, crossed by relatively strong mean motion resonances on both sides very close to the parent body, are exactly the inverse of 'limiting' diameters in the a versus $1/D$ plane. This result uncovers a novel interesting property of asteroid families' Yarkovsky V-shapes.

Key words. Methods: numerical − Methods: data analysis − Celestial mechanics − Minor planets, asteroids: general

1. INTRODUCTION

Mean motion resonance (MMR) is a gravitational effect and one of the main factors that gives rise to the dynamical chaos in the orbital motion of asteroids in the Solar System (Nesvorný and Morbidelli 1998, Minton and Malhotra 2010, Tsiganis 2010). Many effects of asteroids are dependent on MMRs (refer to Smirnov and Dovgalev (2018) and references therein). Mean motion resonances have a basic role to allow stability against the planetary perturbations, especially for orbits with high inclination (Gallardo 2019).

MMRs can change the asteroid's orbital elements, especially the eccentricity and inclination (Bottke et al. 2002, Carruba et al. 2005, Masiero et al. 2015, Nesvorný et al. 2015). More specifically, MMR induces periodic oscillations in the asteroid semi-major axis around its centre (Nesvorný and Morbidelli 1998).

The Yarkovsky thermal force changes the orbital elements of objects revolving around a body, which is a source of heat (Rubincam 1987, 1995, Bottke et al. 2006, Vokrouhlický et al. 2015). The influence of Yarkovsky force on asteroid's semi-major axis a ($\mathrm{d}a/\mathrm{d}t$) is larger than the change of a due to the close encounters with planets or massive asteroids on very large time-scales (Delisle and Laskar 2012, Carruba et al. 2013). It is well known that the Yarkovsky effect can transport asteroids through the Solar System (Farinella et al. 1998, Morbidelli and Vokrouhlický

2003, Tardioli et al. 2017). Nowadays, the Yarkovsky force is therefore an inevitable force in calculations to understand the long-term dynamics of an asteroid as well as asteroid population.

The interplay between MMR and the Yarkovsky effect is very important, hence it has been the subject of this study. The Yarkovsky effect can drive an asteroid into a MMR (Vokrouhlický and Farinella 2000). The semi-major axis of the asteroid stays almost constant in the resonance, while its eccentricity slowly increases (Wetherill and Williams 1979, Wisdom 1983). Then, the Yarkovsky effect causes a secular (permanent) drift in the semi-major axis of asteroids in resonances. Finally, interactions between MMR and the Yarkovsky effect may result in an important change of the overall Yarkovsky mobility when an asteroid is crossing the mean motion resonance (Vokrouhlický and Brož 2002).

Another important non-gravitational effect – Yarkovsky-O'Keefe-Radzievsky-Paddack (YORP), can initiates a variation of asteroid's rotation rate and obliquity (Rubincam 2000). The YORP is essentially the same physical effect as the Yarkovsky force, but modifies the rotation states of asteroids. In our previous studies (Milić Žitnik and Novaković 2015, 2016, Milić Žitnik 2016, 2018, 2019) we did not take into account the YORP effect, because we had a very large number of test asteroids. The constant semi-major axis drift speed, we used in our papers, should be considered as the long-term average of the Yarkovsky effect, which should be nearly constant for a large enough statistical sample (Ćuk et al. 2015).

It is obvious that the interactions between the Yarkovsky effect and MMRs have a significant influence on the orbital motion of resonant asteroids, thus affecting asteroid families crossed by mean motion resonances. Asteroid families are the results of collisional or cratering events on asteroids – referred to as parent asteroids (Durda et al. 2004, Michel et al. 2015). The members of asteroid families are clustered in their proper orbital elements close to the proper orbital elements of the parent asteroid (Hirayama 1918, Nesvorný et al. 2015). The well known hierarchical clustering method – *HCM* (Zappala et al. 1990, Nesvorný et al. 2015) is usually the employed method for identification of asteroid families, especially for the old ones.

Asteroid family members disperse with time. It was initially considered that asteroid fragments remained motionless in the proper orbital elements space after collisional or cratering events. Then, in order to explain the dispersion of asteroid family members, it was necessary that large ejection velocities exist (Zappalà et al. 1996). Later, it was known that the Yarkovsky effect was mostly a cause of large scattering of asteroids in asteroid families (Michel et al. 2001, Bottke et al. 2001). After an asteroid family forms, the asteroids' orbits change in the space of proper elements because of gravitational and non-gravitational perturbations, which means that asteroid families dynamically evolve (Carruba et al. 2018). A cluster of asteroids is identified as a family if its boundary in the $(a, 1/D)$ or (a, H) planes has a V-shape which is dependent on the value of the Yarkovsky thermal effect (D is the asteroid diameter, H is the asteroid absolute magnitude) spreading on very large time-scales. The change of members' semi-major axis due to the initial velocity varies with its diameter D as $1/D^\beta$, where the coefficient β is supposed to be very close to 1 (Nesvorný et al. 2002). This causes smaller members to be more disperse than larger ones, so the distribution of an asteroid family resembles the letter "V". The semi-major axis drift rate, da/dt, caused by the Yarkovsky force, is proportional to $1/D$, creating a V-shape in the $(a, 1/D)$ plane with a border defined by a straight line (Milani et al. 2014, Spoto et al. 2015). V-shapes of asteroid families are generally utilized for estimating the age of families (e.g. Spoto et al. 2015, Vokrouhlický et al. 2015). The gradients of the borders of V-shapes reveal the age of an asteroid family (Spoto et al. 2015): with younger families having steeper and older ones shallower gradients.

Recently, Bolin et al. (2018) proposed a connection between the thermal inertia and asteroid diameter D, and revealed that asteroid's Yarkovsky drift rates might have a more complex size dependence than it was initially thought. According to their findings, the family V-shape boundary is curved in the $(a, 1/D)$ plane. Our paper also proposed that in some special cases asteroids are drifting faster with larger diameters than previously considered, decreasing on average the known ages of asteroid families. This occurrence could be connected with the 'limiting' value of the Yarkovsky drift speed we have recently calculated (Milić Žitnik 2019), below which asteroids accelerate motion across MMRs, especially across stronger ones. Also, our 'limiting' value of da/dt could be the 'breakpoint' in changing the V-shape slope of borders of some asteroid families in the $(a, 1/D)$ plane, which is the subject of the present study.

1.1. The 'limiting' value of the Yarkovsky drift speeds

Now, it is necessary to recall our definition of the time interval lead/lag that an asteroid spent in the MMR under the influence of the Yarkovsky drift speed (Milić Žitnik and Novaković 2016):

$$dt_r = \Delta t - \frac{\Delta a}{da/dt}, \qquad (1)$$

where Δt and Δa are defined as $\Delta t = t_2 - t_1$ and $\Delta a = a_2 - a_1$, a_1 and a_2 are the semi-major axes we got from numerical integrations at moments t_1 and t_2 of entering and exiting from the resonance, respectively. We presented orbital evolution of two test asteroids in the (t, a) plane in order to show how we calculated these moments t_1 and t_2 (Fig. 1 and Fig. 2).

Our dt_r measures the time for an asteroid to cross strictly one whole MMR. It is important to say that with Eq. (1) we bypass the problem of need to determine precisely the exiting instant t_2, that exists
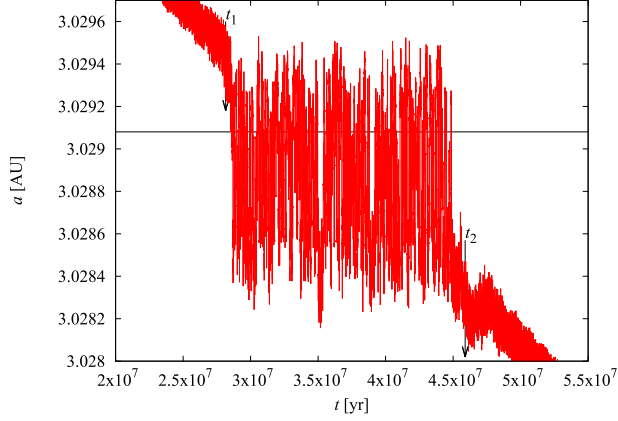
Fig. 1: An example of behaviour of a test asteroid with the Yarkovsky drift speed $da/dt = -6 \times 10^{-5}$ au/Myr, entering our strongest resonance 9:4 with Jupiter at the instant $t_1 = 28153800$ yr and exiting at the instant $t_2 = 45888800$ yr. The horizontal line is the resonance center.
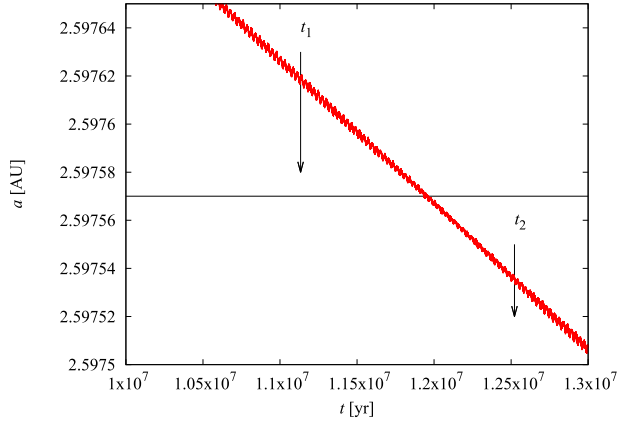

Fig. 2: An example of behaviour of a test asteroid with the Yarkovsky drift speed $da/dt = -6 \times 10^{-5}$ au/Myr, entering our weakest resonance 17:6 with Jupiter at the instant $t_1 = 11419200$ yr and exiting at the instant $t_2 = 12521800$ yr.

only in some cases and, as a consequence, the time interval Δt is not determined precisely enough (Milić Žitnik 2018). This dtr is the time that we obtained by subtracting the time taken for the asteroid to cross the resonance under the influence only of the Yarkovsky drift speed ($\frac{\Delta a}{da/dt}$) from the time that the asteroid spent in the resonance (Δt). In this way, with dt_r we obtained a more objective assessment of the effect of the resonance on the semi-major axis under the influence of the Yarkovsky drift speed.

Furthermore, dt_r measures the speeding up (negative values of dt_r) or slowing down (positive values of dt_r) of the asteroid motion, meaning that a single MMR could either speed up or slow down the drift in the semi-major axis (Milić Žitnik and Novaković 2016). The explanation for these results is

that MMRs have a more powerful influence (large oscillations in semi-major axis of asteroids around resonance's centre) than very small Yarkovsky drift speeds (secular drift in semi-major axis of asteroids) on the motion of resonant asteroids, especially stronger ones. Specifically, all asteroids that crossed over 7:3 with Jupiter had negative average $\langle dt_r \rangle$ values (Milić Žitnik 2018). The resonance 7:3 with Jupiter is very strong, so large oscillations in the semi-major axis often bring asteroids very close to the resonance boundaries and they can more easily and quickly escape from the resonance.

In Milić Žitnik (2019) we calculated that the limiting value of da/dt in the motion of resonant asteroids under the influence of the Yarkovsky effect is at $|-7| \times 10^{-5}$ au/Myr. We examined the characteristics of motion for approximately 60 000 test asteroids with very slow Yarkovsky drift speeds (from -25.8×10^{-5} to -0.7×10^{-5} au/Myr) that crossed over 11 two-body MMRs with Jupiter. Fig. 3 shows asteroids that crossed over 11 MMRs with Jupiter for 4 values of the Yarkovsky drift speeds in the neighbourhood of the 'limiting' Yarkovsky drift speed in the plane average time $\langle dt_r \rangle$ versus strength of resonances SR. Below this value asteroids typically cross quickly over the MMR. This is especially the case in strong resonances (for example: 9:4, 8:3 and 13:6 with Jupiter). The 'limiting' Yarkovsky drift speed represents the threshold below which MMRs have a much more powerful impact on the motion of resonant asteroids and resonant asteroids can more easily escape from MMRs.
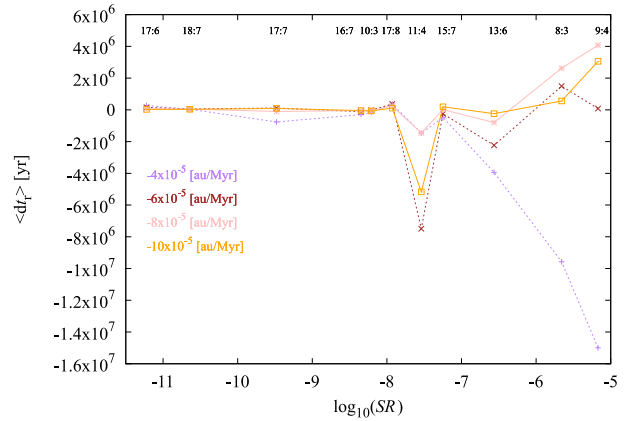
Fig. 3: Changes of the average time $\langle dt_r \rangle$ in MMRs as a function of $\log_{10}(SR)$. The graph shows asteroids that crossed over 11 MMRs for 4 values of the Yarkovsky drift speed in neighbourhood of the 'limiting' Yarkovsky drift speed, -7×10^{-5} au/Myr. Asteroids with -8×10^{-5} and -10×10^{-5} au/Myr (marked with continuous lines) have opposite trend of changing $\langle dt_r \rangle$ (positive values) from asteroids with slower drift speeds (marked with dashed lines – negative values $\langle dt_r \rangle$). This plot represents only the main results in Fig. 2 in Milić Žitnik (2019).

2. METHODS

A key point of this analysis was to find the connection between the 'limiting' Yarkovsky drift speed and asteroid families' Yarkovsky V-shape slope of borders. We have used the catalogue of proper elements for the Main Belt asteroids available at Asteroid Families Portal (AFP)[1]. The catalogue contains proper orbital elements of numbered asteroids and the Main Belt comets, computed numerically by methods of the synthetic theory given by Knežević and Milani (2000, 2003). There were only small differences between the procedure of Knežević and Milani, and the one used to produce the catalogues available at the AFP. In this portal orbits of all asteroids were numerically propagated for 10 Myr and all numerical integrations were made with the same dynamical model that included 7 planets (from Venus to Neptune). All proper elements calculations were executed using the same version of the public $ORBFIT$[2] software (Milani and Nobili 1988). Particularly, in this study we employed the HCM method from the AFP application to generate a list of potential members and interlopers of an asteroid family. Importantly, this method also allowed us to exclude interlopers. This application of the HCM has been recently developed by Radović et al. (2017). Radović et al. (2017) first identified dynamical families using only the proper orbital elements, and then applied physical data to further refine family membership. In their method, physical and spectral properties were used to identify interlopers among asteroids initially linked to a family and to exclude them. At the last step, this method generated a list of family members without potential interlopers that we used in this work.

2.1. Selection of the asteroid families and MMRs

We chose 11 asteroid families to be investigated in this study, which are crossed by strong and/or weak MMRs (2-body and 3-body resonances) and located throughout the Main Belt. The main information about families (name of family, age, number of members), are provided in Table 1. The age estimation with its total uncertainty was taken from Spoto et al. (2015). The number of members without interlopers was obtained using the application HCM (Radović et al. 2017). We defined borders for Yarkovsky V-shape asteroid families as described in Spoto et al. (2015). Our main goal was to visualise the shape of sides of family with sufficient precision for the current study. It is important to note that our borders for the V-shapes families were slightly different from the ones presented in Spoto et al. (2015), because we employed a different algorithm to exclude interlopers of an asteroid family (Radović et al. 2017). Therefore, we obtained a slightly different number of family members than in the study by Spoto et al. (2015).

It is generally known that the asteroids in, or very near, the mean motion and secular resonances can be removed from the asteroid family, which would give rise to an incomplete V-shape i.e. a sharp cut. That was the case for most of our selected families, bounded on one or both V-shape sides by relatively strong resonances. Here are presented 6 such families: Adeona, Eos, Eunomia, Hansa, Hygiea, Koronis (Table 2). Also, these families are very old, with ages between 800 Myr and 2 Gyr. Our other 5 families are relatively young, less than 200 Myr old. Two and three body resonances (Jupiter-Saturn-Asteroid) that cross all 11 families, we obtained by applying numerical methods proposed by Gallardo (2006, 2014). Relatively strong and strong MMRs are written in bold in Table 2. All these strong resonances have enough strength to eject most of the family members. So, the sides of these 6 V-shapes are cut by vertical lines in terms of a, which corresponds to the borders of relatively strong or strong resonances in the $(a, 1/D)$ plane. Also, we took into account the 3-body MMRs. Notwithstanding being generally weaker than the 2-body MMRs, the 3-body MMRs are generating a dynamical features in the asteroidal population, such as chaotic evolutions (Nesvorný and Morbidelli 1998). I have decided to use only the 3-body MMRs with Jupiter and Saturn since they are the most massive planets in the Solar System, thereby are a natural choice.

In Table 3 we provide information about the location and strength of relatively strong MMRs that exist in 6 asteroid families presented in Table 2 which have cut off V-shape sides. Gallardo (2006, 2014) have described the methods for calculation of resonance's strength. These methods are presented as open-source codes on the website http://www.fisica.edu.uy/~gallardo/atlas/. They created tables for the resonance's strength values on certain intervals of semi-major axes for certain eccentricity, inclination and argument of perihelion. We used versions for two-body resonances (called *atlas*) and for three-body resonances (called *atlas3br*) with chosen values $e = 0.1$, $i = 5°$, $\omega = 60°$. Strengths SR for the 2-body and $\Delta\rho$ for the 3-body MMRs are not mutually comparable (private communication, for explanations see Gallardo (2006, 2014)).

2.2. Selection of the fit region, binning and calculation of the 'limiting' diameters

In order to find and define a relation between the 'limiting' value of the Yarkovsky drift speed that we have very recently determined (Milić Žitnik 2019) and the V-shape of the Main Belt asteroid families, we had first to calculate the 'limiting' diameters D, for the left and right V-shape sides. It is known that the Yarkovsky drift rate in semi-major axis can be recalculated for different bulk and surface densities, rotation period, orbit, thermal properties, obliquity etc. (Spoto et al. 2015). With the 'limiting' drift rate using the following scaling formula for the drift rate

---

[1] The Asteroid Families Portal is an online platform that gives tools to study asteroid families (http://asteroids.matf.bg.ac.rs/fam/).

[2] Available from http://adams.dm.unipi.it/orbfit/.

Table 1: The first column contains designation of 11 asteroid families, the second column shows the taxonomic class of asteroid family, the third column shows the origin type, the fourth column shows the age estimation with its total uncertainty taken from Spoto et al. (2015) and the last column shows the number of family members without interlopers generated with the application *HCM* from *AFP* (Radović et al. 2017).

Number/Name	Tax. class	Orig. type	Age (in, out)±Std (Age) [Myr]	No. members
145 Adeona	C	One-sided	(794,/)±(184,/)	2629
221 Eos	S	Fragmentation	(1412, 1537)±(290, 334)	13604
15 Eunomia	S	Cratering	(1955, 1144)±(421, 236)	5837
480 Hansa	S	Fragmentation	(763, 950)±(346, 223)	1399
10 Hygiea	C	Cratering	(1330, 1368)±(300, 329)	6181
158 Koronis	S	Fragmentation	(1792, 1708)±(444, 399)	7240
396 Aeolia	Xe	Young	(100, 91)±(31, 27)	453
606 Brangane	S	Young	(48, 44)±(10, 11)	280
434 Hungaria	Xe	Fragmentation	(208, 205)±(65, 62)	6184
3815 Konig	C	Young	(51, 51)±(14, 14)	523
20 Massalia	S	Cratering	(174, 189)±(35, 41)	7370

Table 2: The first column contains designations of 11 asteroid families and the second column presents the mean motion resonances for the 2- (with Venus, Earth, Mars, Jupiter, Saturn) and the 3-body (Jupiter-Saturn-Asteroid) in these families, that we obtained by applying a numerical methods proposed by Gallardo (2006, 2014). Relatively strong and strong MMRs are written in bold.

Number/Name	Mean motion resonances
145 Adeona	**4:9 M**, 6:13 M, 14:5 J, 7:1 S, 17:6 J, **8:3 J**, **3:7 M**, 2 : -7 J : 4 S, 3:13 E **11:4 J**, 1 : 2 J : -12 S
221 Eos	**9:4 J**, **7:3 J**, 16:7 J, 23:10 J, 4:11 M, **11:5 J**, 6 : -13 J : 1 S, **13:6 J** **15:7 J**, 3 : -1 J : -13 S
15 Eunomia	**11:4 J**, 17:6 J, 14:5 J, 7:15 M, **4:9 M**, **3:7 M**, 6:13 M, **8:3 J**, 16:7 J, 1 : -7 J : 11 S
480 Hansa	**11:4 J**, 6:13 M, 17:6 J, **4:9 M**, 14:5 J, **8:3 J**, 19:7 J, **3:7 M**, 3:13 E
10 Hygiea	**13:6 J**, **9:4 J**, **15:7 J**, **17:8 J**, **11:5 J**, 11:2 S, 24:11 J, **2 : -5 J : 2 S**, 19:9 J, **2:1 J** 21:10 J, 23:11 J, 2 : -7 J : 7 S
158 Koronis	**5:2 J**, 6:1 S, 5:13 M, **12:5 J**, **3 : -9 J : 4 S**, 1:8 V, **1:5 E**, **3:8 M**, 4:11 M, **7:3 J**
396 Aeolia	5:12 M, 21:8 J, 1 : 3 J : -14 S, 13:2 S, 13:5 J, 1 : -1 J : -4 S
606 Brangane	5:11 M, 20:7 J, 23:8 J, 3 : -13 J : 11 S, 7 : -18 J : -5 S, 17:6 J, 1 : 6 J : -22 S
434 Hungaria	5:13 E, 8:11 M, 11:15 M, 2:9 V, 4:11 E, 5:14 E, **2:3 M**
3815 Konig	23:8 J, 7 : -19 J : -3 S, 2 : -11 J : 13 S, 5:11 M, 20:7 J, 7 : -18 J : -5 S
20 Massalia	3:11 E, 1:6 V, 10:3 J, **1:2 M**, 4:15 E, 4:25 V, 23:3 S

(Milani et al. 2014, Chesley et al. 2014, Spoto et al. 2015), we calculated the 'limiting' diameters from (symbols with subscript refer to asteroid (101955) Bennu):

$$\frac{\mathrm{d}a}{\mathrm{d}t} = \frac{\mathrm{d}a}{\mathrm{d}t}\bigg|_B \frac{\sqrt{a_B}(1-e_B^2)}{\sqrt{a}(1-e^2)} \frac{D_B}{D} \frac{\rho_B}{\rho} \frac{\cos(\phi)}{\cos(\phi_B)} \frac{1-A}{1-A_B}. \quad (2)$$

In Eq. (2) the value of da/dt is 7×10^{-5} au/Myr and $\cos(\phi) = \pm 1$ (depending on the OUT/IN side, respectively). In order to find the semi-major axis and eccentricity from the binning left and right side separately, we used the method described in Spoto et al. (2015) as previously explained in this section. The

method for creating bins (1.-4.) and calculation 'limiting' diameters (5.-7.) contains the following steps:

1. At the beginning, we calculated the diameters D ($D = 1329 \times 10^{-H/5}/\sqrt{p_v}$, H and geometric albedo, p_v, were taken from files that were the results of application of the *HCM* method on portal *AFP*). The interval between 0 and the maximum value of $1/D$ was divided into N bins. The number of bins was selected for each family separately, relying on the number of members of the family (greater number of members required greater N);

2. The first bin (the bin with the maximum value of $1/D$) had the highest number of asteroids and the number of asteroids decreased in bins with decreasing $1/D$;

Table 3: In the first column are shown designations of 6 asteroid families, in the second column are relatively strong 2- and 3-body mean motion resonances that crossed these asteroid families, in the third column are presented resonances' locations in terms of synthetic proper semi-major axis, and in the last column are shown their strengths SR (for 2-body) and $\Delta\rho$ (for 3-body) calculated with numerical methods by Gallardo (2006, 2014) with chosen values $e = 0.1$, $i = 5°$ and $\omega = 60°$.

Number/Name	(Relatively) strong MMRs	a_s [au]	SR and $\Delta\rho$
145 Adeona	8:3 J, 3:7 M, 11:4 J, 4:9 M	2.705, 2.680, 2.649, 2.616	2.2E-6, 1.6E-7, 2.9E-8, 4.7E-8
221 Eos	9:4 J, 7:3 J, 11:5 J, 13:6 J, 15:7 J	3.029, 2.957, 3.075, 3.106, 3.129	6.8E-6, 3.5E-5, 1.3E-6, 2.7E-7, 5.6E-8
15 Eunomia	11:4 J, 4:9 M, 8:3 J, 3:7 M	2.649, 2.616, 2.705, 2.680	2.9E-8, 4.7E-8, 2.2E-6, 1.6E-7
480 Hansa	11:4 J, 4:9 M, 8:3 J, 3:7 M	2.649, 2.616, 2.705, 2.680	2.9E-8, 4.7E-8, 2.2E-6, 1.6E-7
10 Hygiea	13:6 J, 9:4 J, 15:7 J, 11:5 J	3.106, 3.029, 3.129, 3.075	2.7E-7, 6.8E-6, 5.6E-8, 1.3E-6
	17:8 J, 2: -5 J : 2 S, 2:1 J	3.147, 3.173, 3.277	1.2E-8, 0.18E-02, 1.99E-02
158 Koronis	5:2 J, 12:5 J, 3 : -9 J : 4 S	2.824, 2.902, 2.851	2. 0E-4, 9.9E-8, 0.5E-3
	1:5 E, 3:8 M, 7:3 J	2.924, 2.930, 2.957	3.9E-8, 2.2E-8, 3.5E-5

3. Standard deviation of the number of asteroids in all bins was computed;

4. The difference between the number of asteroids in two consecutive bins was computed:

4.1. if the difference was less than the standard deviation, the bins were left as they were;

4.2. if the difference was greater than the standard deviation, the differences between numbers of asteroids in consecutive bins was decreased (the total number of family members remains constant). Then, the same procedure was applied to the new bins from step 3.;

5. In the case of low a side the minimum value of synthetic a_s, its $1/D$ and its e_s in each bin was selected. Similarly, for the other side the maximum value of a_s, its $1/D$ and its e_s in each bin was selected. These were the two arrays to be fit (IN and OUT).

6. a_{min}, e_{mean} (arithmetic mean of e_s) for the IN side (from the IN array) and a_{max}, e_{mean} for the OUT side (from the OUT array) was chosen.

7. At the end, using Eq. (2) and values for the orbital elements from step 6, D_{min} (for the IN V-shape side) and D_{max} (for the OUT side) were calculated.

Therefore, D_{min} and D_{max} were not the diameters of an asteroid. They were reference values corresponding to the IN/OUT V-shape side. In our case, they were our 'limiting' diameters $D_{limit} = \{D_{min}, D_{max}\}$ that we calculated with known (101955) Bennu orbital parameters and physical properties (Chesley et al. 2014, Nolan et al. 2013, Emery et al. 2014). The best estimate available for da/dt was exactly the one of asteroid (101955) Bennu, with signal to noise ratio ≈ 200 (Chesley et al. 2014). Recently, Del Vigna et al. (2018) gave estimations of da/dt for approximately 40 near-Earth asteroids, but with poor signal to noise ratio and with no available well known physical parameters in some cases.

3. RESULTS

Table 4 presents our results on final orbital elements a_s and e_{mean} for IN and OUT V-shape sides. Density, ρ, and Bond albedo, $1 - A$, were taken from Spoto et al. (2015) and from files that were the results of the improved HCM method application given on the portal AFP (Radović et al. 2017).

Table 4: In the first column are shown designations of 11 asteroid families, in the second column are presented marks for the left (IN) and the right (OUT) V-shape side of asteroid families, in the third column are shown synthetic proper semi-major axis, minimum value of the left and maximum value of the right side, in the fourth column are the mean values of eccentricity of both sides, the fifth column contains the Bond albedo and the last column shows the density.

Name	Side	a_s [au]	e_{mean}	$1 - A$	ρ [g/cm³]
145 Adeona	IN	2.5428	0.1627	0.98	1.41
	OUT	2.7106	0.1658		
221 Eos	IN	2.9602	0.0725	0.95	2.28
	OUT	3.1399	0.0658		
15 Eunomia	IN	2.5282	0.1503	0.92	2.28
	OUT	2.7098	0.1490		
480 Hansa	IN	2.5377	0.0403	0.91	2.28
	OUT	2.7314	0.0287		
10 Hygiea	IN	3.0183	0.1363	0.98	1.41
	OUT	3.2429	0.1096		
158 Koronis	IN	2.8268	0.0400	0.92	2.28
	OUT	2.9707	0.0723		
396 Aeolia	IN	2.7277	0.1684	0.97	2.75
	OUT	2.7519	0.1669		
606 Brangane	IN	2.5693	0.1805	0.96	2.28
	OUT	2.5953	0.1803		
434 Hungaria	IN	1.8226	0.0598	0.87	2.75
	OUT	2.0188	0.0770		
3815 Konig	IN	2.5584	0.1393	0.98	1.41
	OUT	2.5884	0.1411		
20 Massalia	IN	2.3279	0.1649	0.92	2.28
	OUT	2.4743	0.1615		

Finally, in Table 5 we show the values for 'limiting' diameters, D_{min} and D_{max}. 'Limiting' diameters have very similar values for the IN and OUT side for an asteroid family that follows from the Eq. (2) and from Table 4.

Results from our previous study (Milić Žitnik 2019) showed that below the 'limiting' value of the Yarkovsky drift speed (larger sizes of asteroids $\sim$ smaller Yarkovsky drift speeds), the asteroids accelerated their motion across MMRs, as we have already said. Therefore, this is the 'breakpoint' between the two different 'regimes' of orbital motion of resonant asteroids.

Table 5: The first column contains designations of 11 asteroid families, in the second column are shown marks for the left (IN) and right (OUT) V-shape side of the asteroid family, and in the third column one finds the 'limiting' diameter for the left and right side, calculated via Eq. (2) (Chesley et al. 2014).

Number/Name	Side	D_{limit} [km]
145 Adeona	IN	7.8043
	OUT	7.5668
221 Eos	IN	4.2531
	OUT	4.1256
15 Eunomia	IN	4.5358
	OUT	4.3795
480 Hansa	IN	4.3841
	OUT	4.2224
10 Hygiea	IN	7.1056
	OUT	6.8096
158 Koronis	IN	4.1994
	OUT	4.1114
396 Aeolia	IN	3.8315
	OUT	3.8126
606 Brangane	IN	4.7434
	OUT	4.7193
434 Hungaria	IN	4.0995
	OUT	3.9044
3815 Konig	IN	7.7243
	OUT	7.6834
20 Massalia	IN	4.7494
	OUT	4.6013

In practice, the Yarkovsky effect depends on many parameters. We did not consider here the YORP effect – a 'twin' of the Yarkovsky effect. YORP affects the rotation and spin orientation of asteroids in such a way that it often causes the migration of the spin vector pole towards extreme obliquities measured from the normal to the orbital plane (Vokrouhlický et al. 2015) on a time-scale of the order of a YORP cycle. The duration of a cycle increases with the size of the asteroid: for a given family age, the objects larger than a given value have not had time to be strongly affected by YORP (Paolicchi and Knežević 2016). For this reason, due to the Yarkovsky effect, the YORP changes the evolution of the semi-major axis with time. The clustering of axes causes a clustering in semi-major axis close to the borders of the V-plot of some asteroid families (Vokrouhlický et al. 2006): Yarkovsky/YORP should move small asteroids from the center of the family to more distant semi-major values. So, the YORP effect and other mechanisms that may change the asteroid spin axis orientation (e.g. non-destructive collisions) in general enhance/reduce the efficiency of the Yarkovsky effect and the essence of the influence of the Yarkovsky effect remains the same.

We will show later that the 'limiting' diameter represents exactly the value at which or very near

the V-shape of an old family changes the slope of border, when it is crossed on the same side by strong MMR very close to the parent body, in the $(a, 1/D)$ plane. This effect could be explained by the previously mentioned interaction, between the resonant asteroids that crossed over that strong MMR close to the parent body and the Yarkovsky drift speed, in Milić Žitnik (2019). Therefore, we chose 6 families (ages greater than 200 Myr) crossed by relatively strong and 5 families (ages less than 200 Myr) crossed by weak MMRs near to the parent body. We presented each family in the $(a, 1/D)$ plane with the 'limiting' diameters for the IN/OUT V-shape sides in order to notice and define possible relationships.

In Figs. 4 to 9 we presented old families crossed by relatively strong MMRs in the $(a_{\mathrm{s}}, 1/D)$ plane. The focus here was on relatively strong MMRs located near to the parent body.

The first family presented here (Fig. 4), Adeona, is crossed by relatively strong resonances: 4:9 with Mars, 11:4 with Jupiter, 3:7 with Mars and 8:3 with Jupiter (see in Table 3). Adeona is crossed by strong 8:3 with Jupiter at 2.70470 au on the far right side and by weak 6:13 with Mars at 2.55128 au on the far left side, which define the OUT/IN borders of the V-shape. As one can see, almost all asteroids in the left part of the family crossed over a relatively strong resonance 11:4 with Jupiter at 2.64978 au located very near to the parent body ("PB" is at 2.67267 au). These asteroids with different size of diameters (with different values of the Yarkovsky drift speeds) interacted with 11:4 with Jupiter. The final result of the interaction is that the asteroids with Yarkovsky drift speeds less than 7×10^{-5} au/Myr exited faster from this relatively strong resonance in comparison to the asteroids with the Yarkovsky drift speeds larger than 7×10^{-5} au/Myr. This means that there exist the two different 'regimes' of the asteroid orbital motion. After the asteroids exited from the resonance, they continued orbital motion due to the Yarkovsky force only. At the end, the location of the 'breakpoint' in slope of the V-shape left border could be described by the existing necessary strength of observed interactions between asteroid orbital motion under the influence of the Yarkovsky effect (drift in semi-major axis) and 11:4 with Jupiter (Milić Žitnik 2019) on long time-scales (Adeona is 800 Myr old). Therefore, the inverse 'limiting' value $1/D_{\mathrm{min}}$ is the 'boundary' between the two different 'regimes' of asteroid motion in 11:4 with Jupiter (faster and slower) on the left V-shape side.

Also, almost all asteroids in the right part of the Adeona crossed over relatively strong resonance 3:7 with Mars at 2.68049 au which is located very near to the parent body (right panel in the Fig. 4). These asteroids with different size of diameters (with different values of the Yarkovsky drift speeds) interacted with 3:7 with Mars. Again, the result of the interaction is that the asteroids with Yarkovsky drift speeds less than 7×10^{-5} au/Myr exited faster from this relatively strong resonance in comparison to the asteroids with the Yarkovsky drift speeds higher than 7×10^{-5} au/Myr. So, the location of the 'breakpoint' in slope
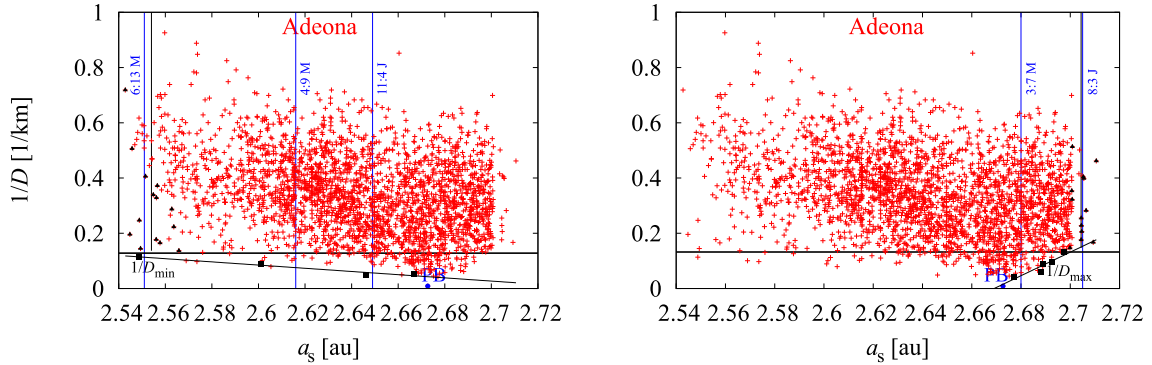
Fig. 4: Family Adeona in the $(a_s, 1/D)$ plane. Crosses are the members of the family. Triangles and squares are both the minimum and maximum values of synthetic semi-major axis a_s for the corresponding inverse of diameter $1/D$ in each bin for the inner and the outer side of the family, respectively (left and right panel). Horizontal lines represent the inverse values of the corresponding 'limiting' diameters $1/D_{min}$ and $1/D_{max}$ for both sides calculated via the scaling formula for da/dt (Milani et al. 2014, Chesley et al. 2014, Spoto et al. 2015) with the 'limiting' value 7×10^{-5} au/Myr of the Yarkovsky drift speed. Oblique and vertical lines represent the best data fit in order to visualise the shape of family borders, above and below the inverse 'limiting' values $1/D_{limit}$, and therefore to find a relationship between the 'limiting' diameters and the slopes of V-shape borders. Abbreviation "PB" denotes the parent body of family. See the text for further explanation.

on the V-shape right border could be explained by the existing necessary strength of observed interactions between the asteroid orbital motion under the influence of the Yarkovsky effect and relatively strong 3:7 with Mars (Milić Žitnik 2019). Therefore, the inverse 'limiting' value $1/D_{max}$ is the 'boundary' between the two different 'regimes' of asteroid motion on the right V-shape side.

A very important fact to observe here is that the Adeona is an old family – approximately 800 Myr old (Spoto et al. 2015). So, the result of the interaction between asteroid's orbital motion due to the Yarkovsky effect and relatively strong MMRs (located very near to the parent body on the both sides: 11:4 with Jupiter and 3:7 with Mars) had enough time to be expressed in this family. So, family members had a great spread in semi-major axis on long time-scales and whether strong or weak resonance cut V-shape borders (weak 6:13 with Mars on the left and strong 8:3 with Jupiter on the right border), the result of the interaction between asteroid's orbital motion due to the Yarkovsky effect and relatively strong MMRs near to the parent body is obvious. Most of the family members (both with small and large diameters) crossed over relatively strong MMRs, located very near on the both sides to the parent body, and after that they had enough time to spread in a (Fig. 4). The time is an important factor, especially for asteroids with very small Yarkovsky drift speeds (asteroids with large diameters) and for asteroid families. The location of the 'breakpoint' in slope of borders in Adeona could be described by the existing necessary strength of interactions between asteroid orbital motion under the influence of the Yarkovsky effect and strong MMRs (located very near to the parent body on the both sides) on long time-scales. Therefore, it was evident here that the inverse of 'limiting' values $1/D_{limit}$ represents the 'boundaries' between

the two different 'regimes' of asteroids' motion on the both V-shape sides. The conclusion is that the inverse of the 'limiting' diameter $1/D_{limit}$ exists exactly at the place where the oblique shape transformed to the vertical one on the same side of the family (left and right panel in Fig. 4), when there exists a necessary strength of interactions between the asteroid orbital motion due to the Yarkovsky effect and relatively strong MMRs on both sides very near to the parent body on long time-scales. That is precisely the place of change of the V-shape border slope when a strong or relatively strong MMR is located very near to the parent body on the same side in the old asteroid family.

Family Eos is crossed by relatively strong resonances: 9:4 with Jupiter, 11:5 with Jupiter, 7:3 with Jupiter, 13:6 with Jupiter and 15:7 with Jupiter (see in Table 3). Eos is crossed by strong 7:3 with Jupiter at 2.95652 au on the left border and by relatively strong 15:7 with Jupiter at 3.12923 au on the right V-shape border (Fig. 5). Almost all asteroids in the right part of the family were crossed over strong resonance 9:4 with Jupiter at 3.02908 au which is located very near to the parent body (at 3.01271 au). Eos is a very old family – approximately 1500 Myr old (Spoto et al. 2015). Most of the family members (with different size of diameters) crossed over 9:4 with Jupiter and after that they had enough time to spread in a. The result of the interaction is that the asteroids with Yarkovsky drift speeds less than 7×10^{-5} au/Myr exited faster from this strong resonance than the asteroids with Yarkovsky drift speeds larger than 7×10^{-5} au/Myr. After the asteroids exited from the 9:4 with Jupiter, they continued the orbital motion due to the Yarkovsky force only. The location of the 'breakpoint' on the right V-shape border could be described as the result of the existing necessary strength of interaction between the asteroid
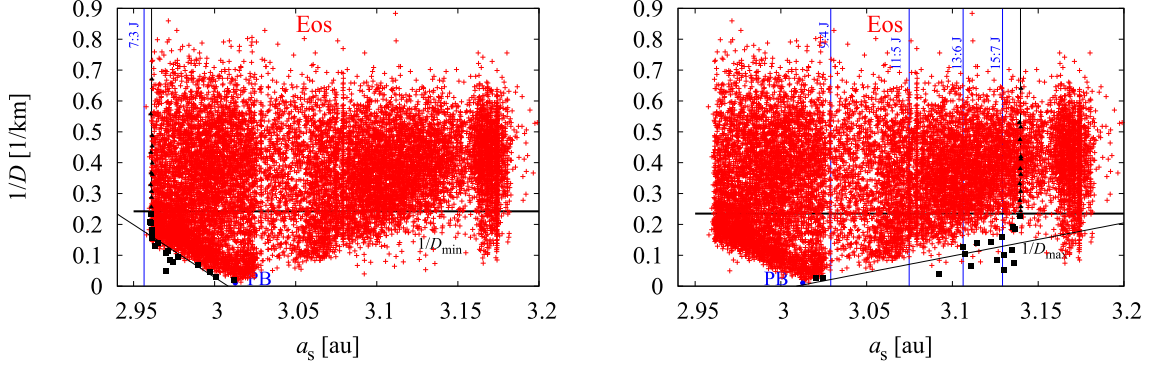
Fig. 5: The same as in Fig. 4, for the family Eos. See the text for explanation.
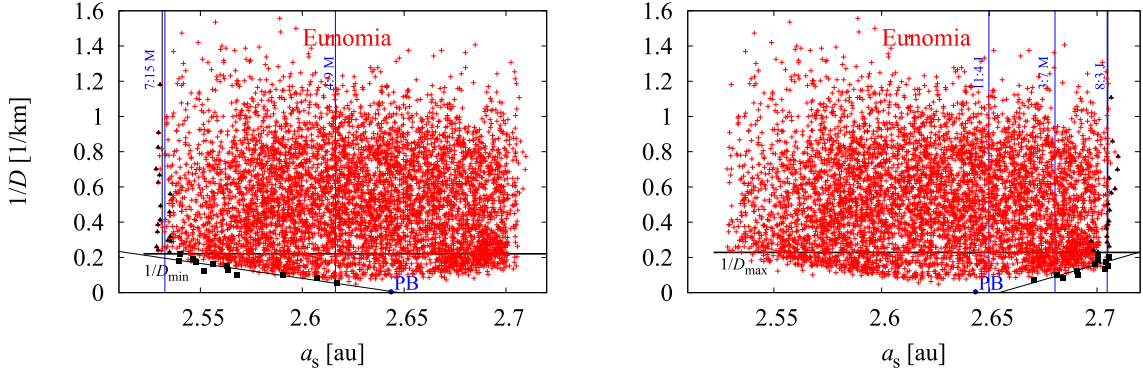
Fig. 6: The same as in Fig. 4, for the family Eunomia. See the text for explanation.

orbital motion under the influence of the Yarkovsky effect and strong 9:4 with Jupiter (Milić Žitnik 2019). Also, the observed interaction had enough time to be expressed in this family. The family members had a great spread in semi-major axis after they exited from 9:4 with Jupiter. Therefore, the inverse 'limiting' value $1/D_{max}$ is exactly the 'boundary' between the two different 'regimes' of the asteroid motion on the right V-shape side. Eos is not crossed by strong or relatively strong resonances on the left side of the V-shape near to the parent body. So, on the left side does not exist the observed interaction between asteroid orbital motion due to the Yarkovsky effect and relatively strong resonance does not exist. This is the explanation of not matching locations of the 'breakpoint' on the left border of the V-shape and inverse of the 'limiting' diameter $1/D_{min}$.

Family Eunomia is crossed by relatively strong resonances: 11:4 with Jupiter, 4:9 with Mars, 8:3 with Jupiter and 3:7 with Mars (see in Table 3). Eunomia is crossed by strong 8:3 with Jupiter at 2.70470 au on the right border and by weak 7:15 with Mars at 2.53255 au on the left V-shape border (Fig. 6). Almost all asteroids (with different size of diameters) on the right side of the family crossed over relatively strong resonance 11:4 with Jupiter at 2.64978 au which is located very close to the parent body (at 2.64357 au). The location of the 'breakpoint' on the right V-shape border could be described by existing the necessary strength of interactions between

asteroid orbital motion due to the Yarkovsky effect and 11:4 with Jupiter (Milić Žitnik 2019). Therefore, the inverse 'limiting' value $1/D_{max}$ is exactly the 'boundary' between the two different 'regimes' of asteroid motion on the right V-shape side. Eunomia is a very old family – approximately 2000 Myr old (Spoto et al. 2015). Also, the observed interaction had enough time to be expressed in this family. Almost all asteroids on the left side of the family crossed over the relatively strong resonance 4:9 with Mars at 2.61628 au which is located very close to the parent body. So, the location of the 'breakpoint' on the left V-shape border could be described as the result of existing the necessary strength of interactions between the asteroid orbital motion under the influence of the Yarkovsky effect and 4:9 with Mars (Milić Žitnik 2019) on long time-scales. Therefore, the inverse 'limiting' value $1/D_{min}$ is exactly the 'boundary' between the two different 'regimes' of asteroid motion on the left V-shape side.

Family Hansa is crossed by strong and relatively strong resonances: 11:4 with Jupiter, 4:9 with Mars, 8:3 with Jupiter and 3:7 with Mars (see in Table 3). Hansa is crossed by strong 8:3 with Jupiter at 2.70470 au on the right border and by weak 6:13 with Mars at 2.55128 au on the left V-shape border (Fig. 7). Almost all asteroids on the left side of the family crossed over relatively strong resonance 4:9 with Mars at 2.61628 au which is located very near to the parent body (at 2.64407 au). The location of the 'break-
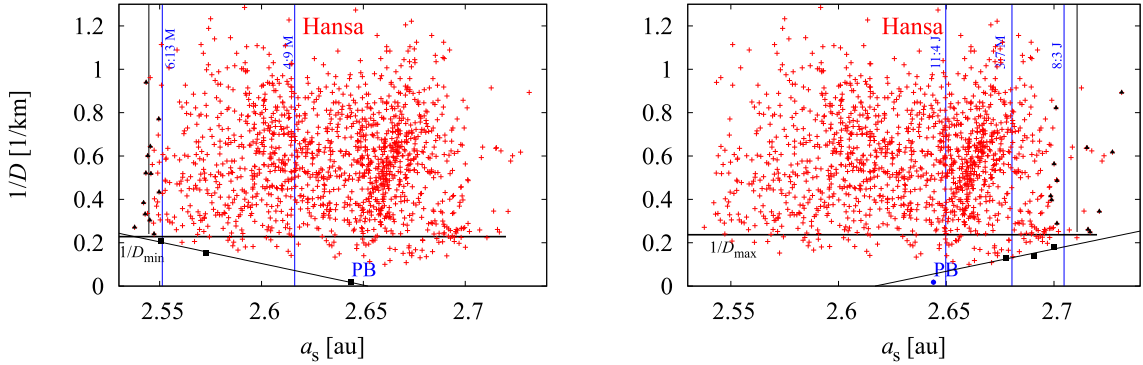
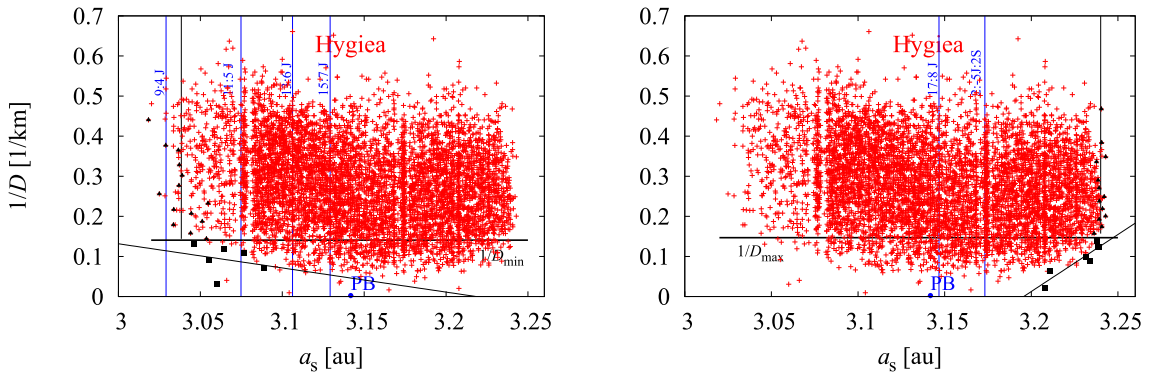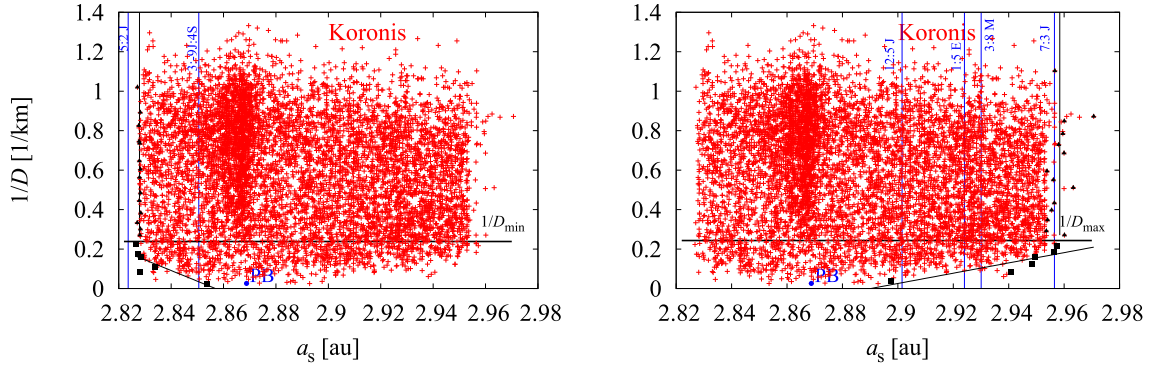**Fig. 7**: The same as in Fig. 4, for the family Hansa. See the text for explanation.

Fig. 8: The same as in Fig. 4, for the family Hygiea. See the text for explanation.

point' on the left V-shape border could be described as the result of existing the necessary strength of interactions between asteroid orbital motion under the influence of the Yarkovsky effect and 4:9 with Mars (Milić Žitnik 2019). Hansa is an old family – approximately 800 Myr old (Spoto et al. 2015). Also, the observed interaction had enough time to be expressed in this family. The family members had a great spread in semi-major axis after they came out from 4:9 with Mars. Therefore, the inverse 'limiting' value $1/D_{min}$ is exactly the 'boundary' between the two different 'regimes' of asteroid motion on the left V-shape side. Almost all asteroids on the right side of the family crossed over relatively strong resonance 11:4 with Jupiter at 2.64978 au which is located very near to the parent body. Again, the location of the 'breakpoint' on the right V-shape border could be described by existing the necessary strength of interactions between the asteroid orbital motion under the influence of the Yarkovsky effect and 11:4 with Jupiter (Milić Žitnik 2019) on long time-scales. Therefore, the inverse 'limiting' value $1/D_{max}$ is exactly the 'boundary' between the two different 'regimes' of asteroid motion on the right V-shape side.

Family Hygiea is crossed by strong and relatively strong resonances: 9:4 with Jupiter, 13:6 with Jupiter, 15:7 with Jupiter, 11:5 with Jupiter, 2:-5:2 with Jupiter and Saturn, 17:8 with Jupiter and 2:1 with Jupiter (see in Table 3). Hygiea is crossed by

strong 9:4 with Jupiter at 3.02908 au on the left border and by very strong 2:1 with Jupiter at 3.27652 au on the right V-shape border (Fig. 8). Almost all asteroids on the left side of the family crossed over relatively strong resonance 15:7 with Jupiter at 3.12923 au which is located very near to the parent body (at 3.14180 au). The location of the 'breakpoint' on the left V-shape border could be described as the result of existing the necessary strength of interactions between the asteroid orbital motion under the influence of the Yarkovsky effect and 15:7 with Jupiter (Milić Žitnik 2019). Hygiea is a very old family – approximately 1300 Myr old (Spoto et al. 2015). The observed interaction had enough time to be expressed in this very old family. Therefore, the inverse 'limiting' value $1/D_{min}$ is exactly the 'boundary' between the two different 'regimes' of asteroid motion on the left V-shape side. Almost all asteroids on the right side of the family crossed over relatively strong resonance 17:8 with Jupiter at 3.14673 au which is located very near to the parent body. Again, the location of the 'breakpoint' on the right V-shape border could be described by existing the necessary strength of interactions between the asteroid orbital motion due to the Yarkovsky effect and 17:8 with Jupiter (Milić Žitnik 2019) on long time-scales. Therefore, the inverse 'limiting' value $1/D_{max}$ is exactly the 'boundary' between the two different 'regimes' of asteroid motion on the right V-shape side.
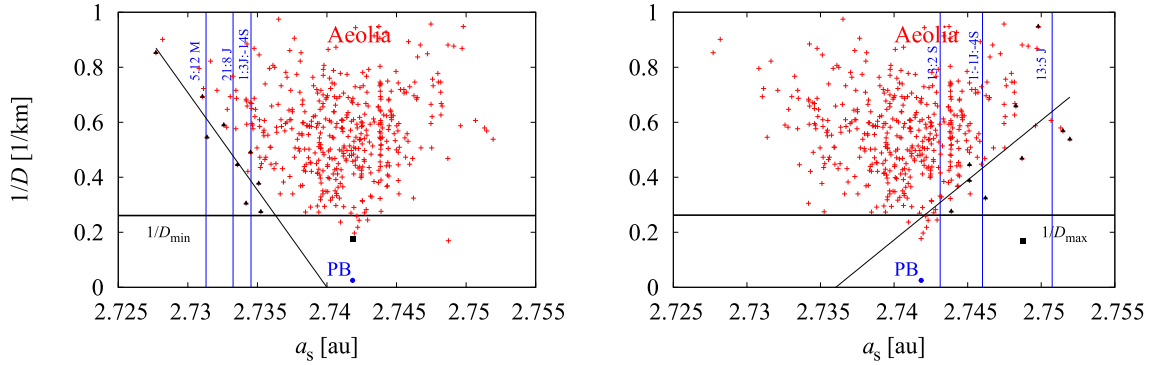
Fig. 9: The same as in Fig. 4, for the family Koronis. See the text for explanation.

Family Koronis is crossed by strong and relatively strong resonances: 5:2 with Jupiter, 12:5 with Jupiter, 1:5 with Earth, 3:8 with Mars, 7:3 with Jupiter and 3:-9:4 with Jupiter and Saturn (see in Table 3). Koronis is crossed by very strong 5:2 with Jupiter at 2.82362 au on the left border and by strong 7:3 with Jupiter at 2.95652 au on the right V-shape border (Fig. 9). Almost all asteroids on the left side of the family crossed over relatively strong resonance 3:-9:4 with Jupiter and Saturn at 2.85057 au which is located near to the parent body (at 2.86878 au). The location of the 'breakpoint' on the left V-shape border could be described as the result of existing the necessary strength of interactions between the asteroid orbital motion under the influence of the Yarkovsky effect and relatively strong 3:-9:4 with Jupiter and Saturn (Milić Žitnik 2019). Koronis is a very old family – approximately 1700 Myr old (Spoto et al. 2015). So, the result of the interaction between asteroid orbital motion due to the Yarkovsky effect and relatively strong MMR near to the parent body had enough time to be expressed in this family. The family members had a great spread in semi-major axis after they exited from the 3:-9:4 with Jupiter and Saturn on long time-scales. Therefore, the inverse 'limiting' value $1/D_{min}$ is exactly the 'boundary' between the two different 'regimes' of asteroid motion on the left V-shape side. Almost all asteroids on the right side of the family crossed over relatively strong resonance 12:5 with Jupiter at 2.90151 au which is located near to the parent body. Again, the location of the 'breakpoint' on the right V-shape border could be described by existing the necessary strength of interactions between the asteroid orbital motion under the influence of the Yarkovsky effect and 12:5 with Jupiter (Milić Žitnik 2019) on long time-scales. Therefore, the inverse 'limiting' value $1/D_{max}$ is exactly the 'boundary' between the two different 'regimes' of asteroid motion on the right V-shape side.

Further, we characterized young or relatively young five families (Figs. 10 to 14) that are crossed only by weak mean motion resonances (except the family Massalia) near to the parent body. From the results presented in Figs. 10 to 14, it is noticeable that the inverse of the 'limiting' value $1/D_{limit}$ in the (a_s, $1/D$) plane does not indicate the 'boundary' in V-shape borders. In Figs. 10 to 13 there were no two different 'regimes' of asteroid motion. This case could be explained by the absence of strong MMRs located near to the parent body (situation contrary to the previous 6 families) – the absence of interaction between asteroid orbital motion under the influence of the Yarkovsky effect (drift in semi-major axis) and strong MMRs (Milić Žitnik 2019). In Fig. 14 (family Massalia) there exists one relatively strong MMR (1:2 with Mars) very near to the parent body. The key factor in spreading of asteroid families is time, as it is known. Massalia is a relatively young family (see in Table 1). So, the result of the interaction between the asteroid orbital motion due to the Yarkovsky effect and relatively strong 1:2 with Mars near to the parent body did not have enough time to be expressed in this family. The family members did not have enough large spread in semi-major axis after they exited from the 1:2 with Mars. Of course, if there was a stronger resonance instead of 1:2 with Mars very near to the parent body, then the observed interaction would have become expressed in this family on time-scale of 200 Myr (the age of Massalia). The conclusion here is: the inverse of the 'limiting' diameters $1/D_{limit}$ was not at the place where oblique shapes transform to the vertical ones. In these five families there exist only oblique lines that represent the best fit data on both V-shape sides (see Figs. 10 to 14).

Family Aeolia is not crossed by strong MMRs (see in Table 2) near to the parent body, only by weak MMRs. So, in Aeolia does not exist the observed interaction between the asteroid orbital motion under the influence of the Yarkovsky effect and relatively strong MMR near to the parent body (Fig. 10). Further, Aeolia is a young family – approximately 100 Myr old (Spoto et al. 2015). Inverse of the 'limiting' value $1/D_{limit}$ is not the 'boundary' between the two different 'regimes' of asteroid motion on the same side of the V-shape family. Here there exist only oblique lines that represent the best fit data on both V-shape sides – one 'regime' of asteroids' motion. In Aeolia it is obvious that a statistically insignificant number of asteroids are below the $1/D_{limit}$.

Fig. 10: The same as in Fig. 4, for the family Aeolia. See the text for explanation.
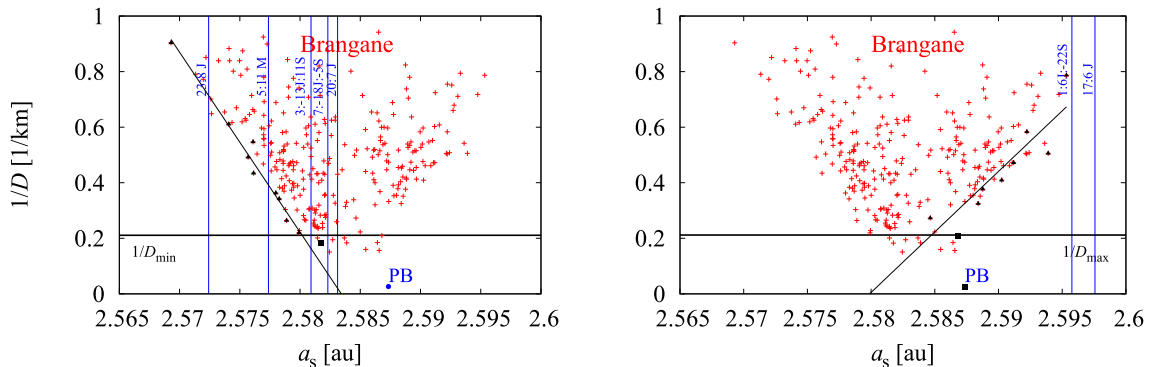
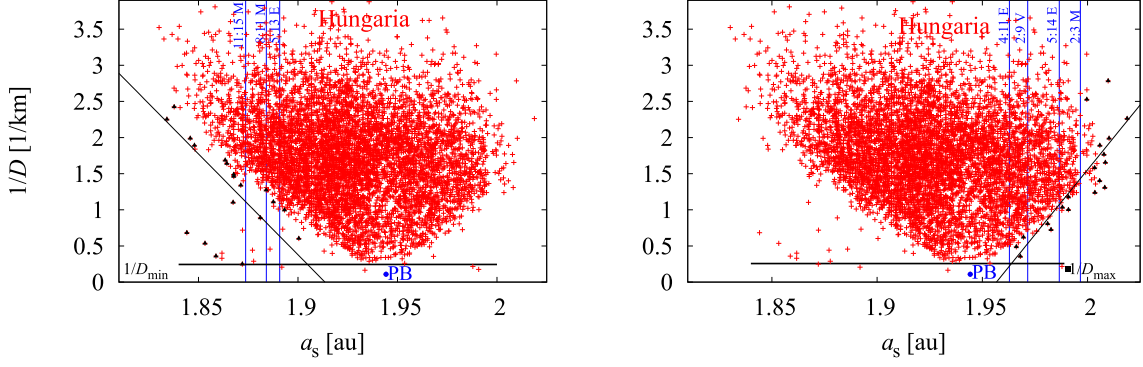**Fig. 11**: The same as in Fig. 4, for the family Brangane. See the text for explanation.

Family Brangane is not crossed by relatively strong resonances near to the parent body, only by weak MMRs (see in Table 2). So, there does not exist the observed interaction between asteroid orbital motion due to the Yarkovsky effect and relatively strong MMR near to the parent body (Fig. 11). Also, Brangane is a very young family – approximately 50 Myr old (Spoto et al. 2015). Therefore, the inverse of the 'limiting' value $1/D_{limit}$ is not the 'boundary' between the two different 'regimes' of asteroid motion on the same side of the V-shape family. Here, there exist only the oblique lines that represent the best fit data on both V-shape sides – one 'regime' of asteroids' motion. In Brangane, it is obvious that very few asteroids are below $1/D_{limit}$.

Family Hungaria is crossed only by weak MMRs near to the parent body and on the left V-shape border is crossed by relatively strong 2:3 with Mars at 1.99660 au (see in Table 2). Also, Hungaria is a relatively young family – approximately 200 Myr old (Spoto et al. 2015). So, in Hungaria the observed interaction between asteroid orbital motion under the influence of the Yarkovsky effect and relatively strong MMRs near to the parent body does not exist (Fig. 12). Therefore, the inverse of 'limiting' value $1/D_{limit}$ is not the 'boundary' between the two different 'regimes' of asteroid orbital motion on both V-shape sides. Here there exist only the oblique lines that represent the best fit data on both sides – one 'regime' of asteroids' motion. In Hungaria, it is obvious that a statistically insignificant number of

asteroids are below $1/D_{limit}$.

Family Konig is not crossed by relatively strong resonances near to the parent body, only by weak MMRs (see in Table 2). So, there does not exist the observed interaction between asteroid orbital motion under the influence of the Yarkovsky effect and relatively strong MMRs near to the parent body (Fig. 13). Also, Konig is a very young family – approximately 50 Myr old (Spoto et al. 2015). Therefore, the inverse of 'limiting' value $1/D_{limit}$ is not the 'boundary' between the two different 'regimes' of asteroid motion on both V-shape sides. Here, there exist only the oblique lines that represent the best fit data on both V-shape sides – one 'regime' of asteroids' motion. In Konig it is obvious that a statistically insignificant number of asteroids are below $1/D_{limit}$.

Family Massalia is crossed by weak MMRs (3:11 with Earth, 4:25 with Venus, 23:3 with Saturn etc.) and by relatively strong 1:2 with Mrs (see in Table 2). Almost all asteroids on the right side of the family crossed over relatively strong resonance 1:2 with Mars at 2.41871 au ($SR = 4.86 \times 10^{-6}$) which is located very near to the parent body (at 2.40863 au) (Fig. 14). The next very important fact about Massalia that is a relatively young family – approximately 180 Myr (Spoto et al. 2015). It means that members of the family Massalia did not have enough time to spread in proper a under the influence of the Yarkovsky effect. Massalia members did not have enough large spread in semi-major axis after they ex-

Fig. 12: The same as in Fig. 4, for the family Hungaria. See the text for explanation.
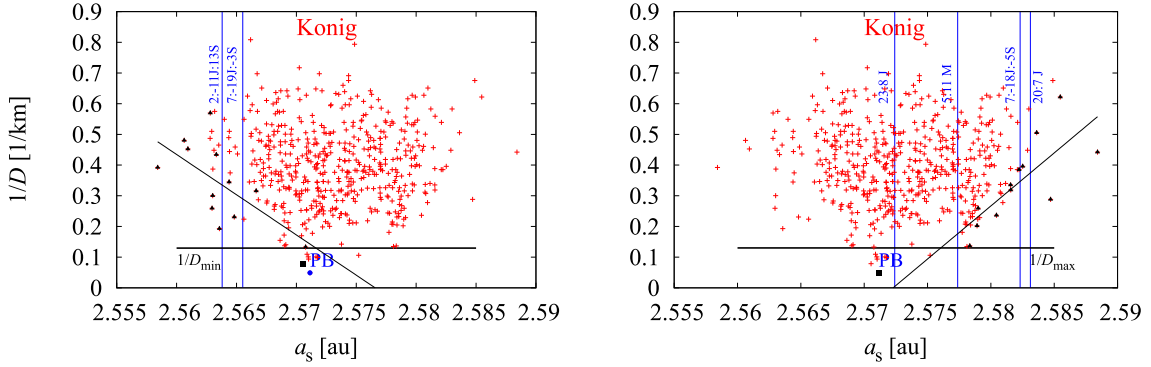
Fig. 13: The same as in Fig. 4, for the family Konig. See the text for explanation.
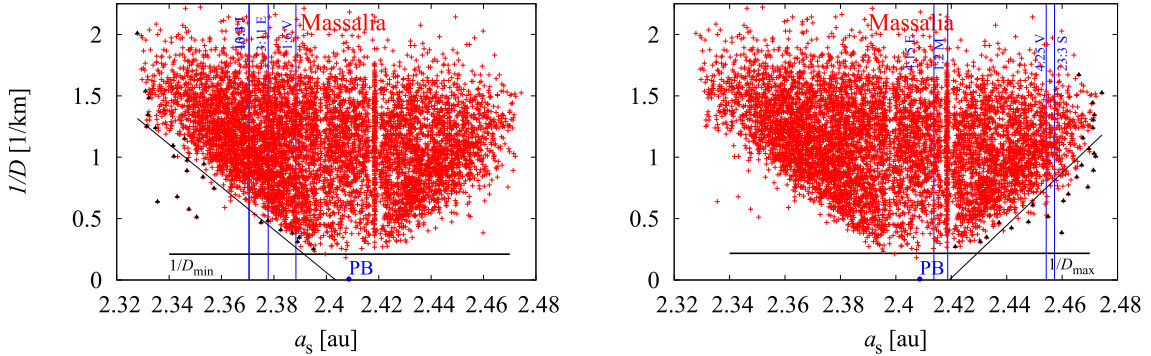
Fig. 14: The same as in Fig. 4, for the family Massalia. See the text for explanation.

ited from the 1:2 with Mars. So, the observed interaction between asteroid orbital motion under the influence of the Yarkovsky effect and relatively strong MMR did not have enough time to be expressed in this family. We will compare it to the situation with Adeona (see Fig. 4, left panel). In Adeona almost all asteroids on the left side of the family crossed over relatively strong resonance 11:4 with Jupiter which is located very near to the parent body. The difference is that Adeona is an old family – approximately 800 Myr (Spoto et al. 2015). So, the observed interaction between asteroid orbital motion due to the Yarkovsky effect and relatively strong MMR near to the parent body had enough time to be expressed in an old family, contrary to the young Massalia. There-

fore, the inverse of the 'limiting' value $1/D_{\mathrm{limit}}$ is not the 'boundary' between the two different 'regimes' of asteroid motion on the same side of the V-shape Massalia. Here, there exist only the oblique lines that represent the best fit data on both V-shape sides.

The fit equations were shown in Figs. 4 to 14 with oblique and vertical lines, which clearly visualise the V-shape sides of asteroid families.

When strong MMRs cross sides of families in the $(a_{\mathrm{s}}, 1/D)$ plane, the best fit equation could be defined by a vertical line:

$$y_{\mathrm{fit1}} = \sum_{i=1}^{n} a_i/n, \qquad (3)$$

Table 6: In the first column are shown designations of 11 asteroid families, in the second column are presented marks of the left and right V-shape sides (above and below the 'limiting' diameters) and in the last column are fit equations with coefficients and fit errors for both sides (y_{fit1} [au], y_{fit2} [1/km], x [au], a [1/km/au], b [1/km].

Number/Name	Side	Fit equations (coefficients and fit errors)
145 Adeona	IN 1	$y_{fit1} = \sum_{i=1}^{n} a_i/n = 2.554$ au
	IN 2	$y_{fit2} = ax + b$ $\quad$ ($a = -0.58 \pm 0.094, b = 1.59 \pm 0.245$)
	OUT 1	$y_{fit1} = \sum_{i=1}^{n} a_i/n = 2.704$ au
	OUT 2	$y_{fit2} = ax + b$ $\quad$ ($a = 4.26 \pm 0.919, b = -11.37 \pm 2.471$)
221 Eos	IN 1	$y_{fit1} = \sum_{i=1}^{n} a_i/n = 2.961$ au
	IN 2	$y_{fit2} = ax + b$ $\quad$ ($a = -3.42 \pm 0.567, b = 10.27 \pm 1.685$)
	OUT 1	$y_{fit1} = \sum_{i=1}^{n} a_i/n = 3.140$ au
	OUT 2	$y_{fit2} = ax + b$ $\quad$ ($a = 1.07 \pm 0.325, b = -3.23 \pm 1.012$)
15 Eunomia	IN 1	$y_{fit1} = \sum_{i=1}^{n} a_i/n = 2.531$ au
	IN 2	$y_{fit2} = ax + b$ $\quad$ ($a = -1.70 \pm 0.266, b = 4.49 \pm 0.681$)
	OUT 1	$y_{fit1} = \sum_{i=1}^{n} a_i/n = 2.705$ au
	OUT 2	$y_{fit2} = ax + b$ $\quad$ ($a = 3.52 \pm 0.734, b = -9.34 \pm 1.978$)
480 Hansa	IN 1	$y_{fit1} = \sum_{i=1}^{n} a_i/n = 2.545$ au
	IN 2	$y_{fit2} = ax + b$ $\quad$ ($a = -1.99 \pm 0.117, b = 5.28 \pm 0.302$)
	OUT 1	$y_{fit1} = \sum_{i=1}^{n} a_i/n = 2.711$ au
	OUT 2	$y_{fit2} = ax + b$ $\quad$ ($a = 2.06 \pm 1.010, b = -5.40 \pm 2.715$)
10 Hygiea	IN 1	$y_{fit1} = \sum_{i=1}^{n} a_i/n = 3.038$ au
	IN 2	$y_{fit2} = ax + b$ $\quad$ ($a = -0.60 \pm 1.144, b = 1.94 \pm 3.506$)
	OUT 1	$y_{fit1} = \sum_{i=1}^{n} a_i/n = 3.240$ au
	OUT 2	$y_{fit2} = ax + b$ $\quad$ ($a = 2.84 \pm 0.507, b = -9.09 \pm 1.636$)
158 Koronis	IN 1	$y_{fit1} = \sum_{i=1}^{n} a_i/n = 2.830$ au
	IN 2	$y_{fit2} = ax + b$ $\quad$ ($a = -5.40 \pm 2.111, b = 15.43 \pm 5.981$)
	OUT 1	$y_{fit1} = \sum_{i=1}^{n} a_i/n = 2.958$ au
	OUT 2	$y_{fit2} = ax + b$ $\quad$ ($a = 2.61 \pm 0.734, b = -7.53 \pm 2.160$)
396 Aeolia	IN	$y_{fit2} = ax + b$ $\quad$ ($a = -70.82 \pm 10.760, b = 194.04 \pm 29.400$)
	OUT	$y_{fit2} = ax + b$ $\quad$ ($a = 43.48 \pm 20.530, b = -118.95 \pm 56.400$)
606 Brangane	IN	$y_{fit2} = ax + b$ $\quad$ ($a = -64.79 \pm 3.764, b = 167.37 \pm 9.697$)
	OUT	$y_{fit2} = ax + b$ $\quad$ ($a = 43.57 \pm 8.504, b = -112.42 \pm 22.030$)
434 Hungaria	IN	$y_{fit2} = ax + b$ $\quad$ ($a = -27.89 \pm 7.689, b = 53.373 \pm 14.330$)
	OUT	$y_{fit2} = ax + b$ $\quad$ ($a = 35.90 \pm 5.789, b = -70.242 \pm 11.550$)
3815 Konig	IN	$y_{fit2} = ax + b$ $\quad$ ($a = -26.22 \pm 10.070, b = 67.54 \pm 25.810$)
	OUT	$y_{fit2} = ax + b$ $\quad$ ($a = 34.56 \pm 9.396, b = -88.91 \pm 24.260$)
20 Massalia	IN	$y_{fit2} = ax + b$ $\quad$ ($a = -17.38 \pm 2.397, b = 41.78 \pm 5.642$)
	OUT	$y_{fit2} = ax + b$ $\quad$ ($a = 21.43 \pm 3.369, b = -51.84 \pm 8.285$)

where y_{fit1} is the arithmetic mean of minimum/maximum of synthetic semi-major axes a_i in n corresponding bins for the IN/OUT side, respectively, for asteroids with diameters smaller than the 'limiting'.

When only the weak MMRs cross sides of families in the $(a_s, 1/D)$ plane, the best fit equation for whole side is linear that could be defined by:

$$y_{fit2} = ax + b, \qquad (4)$$

where $\{y_{fit2}, x\}$ is a pair of inverse diameters $1/D$ and their synthetic semi-major axes a_s for the IN/OUT side. The Eq. (4) is also the best fit equation, in this study, for asteroids with diameters greater than the 'limiting' when strong MMRs cross sides of families.

In Table 6 we presented the fit equations with coefficients and their fit errors for the IN/OUT side for all 11 families. However, it is noticeable that, in all presented figures, there is a relatively large dispersion of values around vertical lines (Eq. (3)), which did not affect the data interpretation. On the contrary, in Table 6 there are presented relatively small fit errors for coefficients a and b of linear equation (Eq. (4)).

Finally, it can be concluded that resonant asteroids with greater sizes than the 'limiting' diameters (asteroids below the $1/D_{limit}$ in the a versus $1/D$ plane) that crossed over relatively strong MMRs, have faster orbital motion than what has been considered to date. This was our conclusion presented in

Milić Žitnik (2019), but now this is done in terms of the 'limiting' diameters. Also, our finding to some extent is in agreement with the conclusion derived in the previous study by Bolin et al. (2018), stating that asteroids are drifting faster at larger sizes (equivalently to smaller inverse sizes $1/D$), decreasing on average the known ages of asteroid families.

4. SUMMARY AND CONCLUSIONS

We here presented a new point of view on the Yarkovsky V-shape asteroid family. It is well known that on the V-shape is influenced by the initial spreading of family member's orbital elements caused by the initial ejection of member, close encounters with massive asteroids, the Yarkovsky effect, mean motion resonances, secular resonances etc. In this study we found another factor that affects the V-shape, one more characteristic about the V-shape. That is the relation between the V-shape borders and the 'limiting' Yarkovsky drift speed in particular cases of asteroid families. We did not consider here the YORP effect, nor other possible mechanisms, that may change the asteroid spin-axis orientation. These effects principally enhance/reduce the efficiency of the Yarkovsky effect (Vokrouhlický et al. 2006).

We have used the known scaling formula to calculate the Yarkovsky drift speed (Milani et al. 2014, Chesley et al. 2014, Spoto et al. 2015) in order to determine the inner and outer 'limiting' diameters (for inner and outer V-shape borders) from the 'limiting' Yarkovsky drift speed, 7×10^{-5} au/Myr, defined in Milić Žitnik (2019). The method was applied to 11 asteroid families of different taxonomic class, origin type and age, located throughout the Main Belt.

In asteroid families, especially in very old ones, which are crossed by strong or relatively strong MMRs on both sides very close to the parent body, at the 'limiting' diameter exists a change in slope of V-shape border in the $(a, 1/D)$ plane. This change of the V-shape could be attributed to the existing necessary strength of interactions between the asteroid orbital motion due to the Yarkovsky effect and relatively strong MMRs (Milić Žitnik 2019). In these families the best fit vertical lines (asteroids with diameters smaller than the 'limiting' diameters) change to the best fit oblique lines (asteroids with diameters larger than the 'limiting' diameters) of family borders in the $(a, 1/D)$ plane. Oblique and vertical lines represent here the best fit data in order to visualise the shape of family sides. Therefore, the inverse of 'limiting' value $1/D_{\text{limit}}$ is the 'breakpoint' between the two different 'regimes' of the resonant asteroid's motion under the influence of the Yarkovsky drift speed (larger and smaller than the 'limiting' drift speed).

In asteroid families, which are crossed only by weak MMRs on both sides very close to the parent body, the 'limiting' Yarkovsky drift speed does not have a role in changing the slope of the V-shape border, because of the absence of appropriate (enough strong) interaction between the asteroid orbital mo-

tion under the influence of the Yarkovsky effect and weak MMRs near to the parent body, as we presented in details in Milić Žitnik (2019). We showed that, in these families, statistically very few asteroids have larger diameters than the 'limiting' diameters, on both V-shape sides. In these families, the whole V-shape sides can be approximated only with the oblique lines in the $(a, 1/D)$ plane and the 'limiting' diameter is not an indicator of 'breakpoint' of the slope, meaning that only one 'regime' of the resonant asteroid's motion exists under the influence of the Yarkovsky effect.

Finally, all our findings of the 'limiting' Yarkovsky drift speed and its 'limiting' diameters are to some extent in good agreement with the recently published result in Bolin et al. (2018): "asteroids are drifting faster at much larger sizes, than it has been previously considered". In our study it holds: resonant asteroids with diameters larger than the 'limiting' diameter (equivalently to smaller Yarkovsky drift speeds than the 'limiting' speed because: $da/dt \sim 1/D$) are drifting faster over relatively strong MMRs.

The main conclusion could be drawn from the present analysis: the location of the inverse of the 'limiting' diameter $1/D_{\text{limit}}$ is exactly at the place of changing the V-shape slope of the border in an old asteroid family which are crossed in the same side by relatively strong MMR, very close to the parent body, in the $(a, 1/D)$ plane.

REFERENCES

Bolin, B. T., Morbidelli, A., and Walsh, K. J. 2018, A&A, 611, A82

Bottke, W. F., Vokrouhlický, D., Brož, M., Nesvorný, D., and Morbidelli, A. 2001, Sci, 294, 1693

Bottke, W. F., Morbidelli, A., Jedicke, R., et al. 2002, Icar, 156, 399

Bottke, W. F. J., Vokrouhlický, D., Rubincam, D. P., and Nesvorný, D. 2006, AREPS, 34, 157

Carruba, V., Michtchenko, T. A., Roig, F., Ferraz-Mello, S., and Nesvorný, D. 2005, A&A, 441, 819

Carruba, V., Huaman, M., Domingos, R. C., and Roig, F. 2013, A&A, 550, A85

Carruba, V., Vokrouhlický, D., and Novaković, B. 2018, P&SS, 157, 72

Chesley, S. R., Farnocchia, D., Nolan, M. C., et al. 2014, Icar, 235, 5

Ćuk, M., Christou, A. A., and Hamilton, D. P. 2015, Icar, 252, 339

Del Vigna, A., Faggioli, L., Milani, A., et al. 2018, A&A, 617, A61

Delisle, J. B. and Laskar, J. 2012, A&A, 540, A118

Durda, D. D., Bottke, W. F., Enke, B. L., et al. 2004, Icar, 170, 243

Emery, J. P., Fernández, Y. R., Kelley, M. S. P., et al. 2014, Icar, 234, 17

Farinella, P., Vokrouhlický, D., and Hartmann, W. K. 1998, Icar, 132, 378

Gallardo, T. 2006, Icar, 184, 29

Gallardo, T. 2014, Icar, 231, 273

Gallardo, T. 2019, MNRAS, 487, 1709

Hirayama, K. 1918, AJ, 31, 185

Knežević, Z. and Milani, A. 2000, CeMDA, 78, 17

Knežević, Z. and Milani, A. 2003, A&A, 403, 1165

Masiero, J. R., DeMeo, F. E., Kasuga, T., and Parker, A. H. 2015, in Asteroids IV, ed. P. Michel, F. E. DeMeo, and W. F. Bottke (Tucson: University of Arizona), 323

Michel, P., Benz, W., Tanga, P., and Richardson, D. C. 2001, Sci, 294, 1696

Michel, P., Richardson, D. C., Durda, D. D., Jutzi, M., and Asphaug, E. 2015, in Asteroids IV, ed. P. Michel, F. E. DeMeo, and W. F. Bottke (Tucson: University of Arizona), 341

Milani, A. and Nobili, A. M. 1988, CeMec, 43, 1

Milani, A., Cellino, A., Knežević, Z., et al. 2014, Icar, 239, 46

Milić Žitnik, I. 2016, SerAJ, 193, 19

Milić Žitnik, I. 2018, POBeo, 98, 153

Milić Žitnik, I. 2019, MNRAS, 486, 2435

Milić Žitnik, I. and Novaković, B. 2015, MNRAS, 451, 2109

Milić Žitnik, I. and Novaković, B. 2016, ApJL, 816, L31

Minton, D. A. and Malhotra, R. 2010, Icar, 207, 744

Morbidelli, A. and Vokrouhlický, D. 2003, Icar, 163, 120

Nesvorný, D. and Morbidelli, A. 1998, AJ, 116, 3029

Nesvorný, D., Bottke, W. F. J., Dones, L., and Levison, H. F. 2002, Natur, 417, 720

Nesvorný, D., Brož, M., and Carruba, V. 2015, in Asteroids IV, ed. P. Michel, F. E. DeMeo, and W. F. Bottke (Tucson: University of Arizona), 297

Nolan, M. C., Magri, C., Howell, E. S., et al. 2013, Icar, 226, 629

Novaković, B., Maurel, C., Tsirvoulis, G., and Knežević, Z. 2015, ApJL, 807, L5

Paolicchi, P. and Knežević, Z. 2016, Icar, 274, 314

Radović, V., Novaković, B., Carruba, V., and Marčeta, D. 2017, MNRAS, 470, 576

Rubincam, D. P. 1987, JGR, 92, 1287

Rubincam, D. P. 1995, JGR, 100, 1585

Rubincam, D. P. 2000, Icar, 148, 2

Smirnov, E. A. and Dovgalev, I. S. 2018, SoSyR, 52, 347

Spoto, F., Milani, A., and Knežević, Z. 2015, Icar, 257, 275

Tardioli, C., Farnocchia, D., Rozitis, B., et al. 2017, A&A, 608, A61

Tsiganis, K. 2010, EPJST, 186, 67

Vokrouhlický, D. and Brož, M. 2002, in Modern Celestial Mechanics: From Theory to Applications (Dordrecht: Kluwer), 467

Vokrouhlický, D. and Farinella, P. 2000, Natur, 407, 606

Vokrouhlický, D., Brož, M., Bottke, W. F., Nesvorný, D., and Morbidelli, A. 2006, Icar, 182, 118

Vokrouhlický, D., Bottke, W. F., Chesley, S. R., Scheeres, D. J., and Statler, T. S. 2015, in Asteroids IV, ed. P. Michel, F. E. DeMeo, and W. F. Bottke (Tucson: University of Arizona), 509

Wetherill, G. W. and Williams, J. G. 1979, in Origin and Distribution of the Elements, ed. L. H. Ahrens, Vol. 34 (Oxford/New York,: Pergamon Press), 19

Wisdom, J. 1983, Icar, 56, 51

Zappala, V., Cellino, A., Farinella, P., and Knezevic, Z. 1990, AJ, 100, 2030

Zappalà, V., Cellino, A., Dell'oro, A., Migliorini, F., and Paolicchi, P. 1996, Icar, 124, 156

ВЕЗА ИЗМЕЂУ 'ГРАНИЧНЕ' БРЗИНЕ ДРИФТА ЈАРКОВСКОГ И V-ОБЛИКА ФАМИЛИЈЕ АСТЕРОИДА

I. Milić Žitnik

Astronomical Observatory, Volgina 7, 11000 Belgrade, Serbia

E–mail: *ivana@aob.rs*

Ефекат Јарковског је једно значајно дејство које се узима у обзир у циљу разумевања дуго-периодичне динамике астероида. Ова негравитациона сила утиче на орбиталне елементе тела који се крећу око извора топлоте, специјално на њихове велике полуосе. На основу недавно дефинисане 'граничне' брзине дрифта Јарковског 7×10^{-5} au/Myr у Milić Žitnik (2019) (испод ове вредности брзине астероиди типично брзо пређу резонанце у средњем кретању), одлучили смо да испитамо везу између V-облика фамилија астероида и 'граничне' брзине промене великих полуоса под утицајем ефекта Јарковског. Користили смо познату скалирајућу формулу за израчунавање брзине дрифта Јарковског (Spoto et al. 2015) у циљу израчунавања унутрашњих и спољашњих 'граничних' пречника (за унутрашње и спољашње границе V-облика) из 'граничних' брзина дрифта Јарковског. Метод је примењен на 11 фамилија астероида различитих таксономских класа, порекла и старости, које се налазе широм Главног прстена астероида. Овде представљамо резултате прорачуна везе између V-облика фамилија астероида (пресечених јаким и/или слабим резонанцама у средњем кретању) и 'граничних' пречника у $(a, 1/D)$ равни. Наш главни закључак је да су 'преломне тачке' у промени V-облика веома старих фамилија астероида, које су пресечене релативно јаким резонанцама у средњем кретању са обе стране врло близу родитељском телу, управо места инверзних 'граничних' пречника у $(a, 1/D)$ равни. Овај резултат осветљава једну занимљиву особину V-облика фамилија астероида.